tvst
Retina

One-Year Progression of Capillary Nonperfusion in Nonproliferative Diabetic Retinopathy Using Noninvasive Imaging: The CHART Study

Inês Pereira Marques [1,2], Débora Reste-Ferreira [1], Torcato Santos [1,2], Luís Mendes [1], Ana Cláudia Rocha [1–3], Francesco Bandello [4], Mariacristina Parravano [5,6], Leonardo Mastropasqua [7], Catherine Creuzot-Garcher [8], Sérgio Leal [9], Fabio Baschiera [9], and José Cunha-Vaz [1,10]

[1] AIBILI—Association for Innovation and Biomedical Research on Light and Image, Coimbra, Portugal
[2] CORC—Coimbra Ophthalmology Reading Centre, Coimbra, Portugal
[3] Center for Translational Health and Medical Biotechnology Research (TBIO)/Health Research Network (RISE-Health), ESS, Polytechnic of Porto, Porto, Portugal
[4] Department of Ophthalmology, Vita-Salute University, San Raffaele Scientific Institute, Milan, Italy
[5] IRCCS Fondazione Bietti, Rome, Italy
[6] UniCamillus-Saint Camillus International University of Health Sciences, Rome, Italy
[7] Excellence Eye Research Centre, Chieti-Pescara, Italy
[8] Department of Ophthalmology, CHU Dijon, Dijon, France
[9] Bayer AG, Basel, Switzerland
[10] Faculty of Medicine, University of Coimbra, Coimbra, Portugal

Correspondence: José Cunha-Vaz, AIBILI—Association for Innovation and Biomedical Research on Light and Image, Edifício Prof. Doutor José Cunha-Vaz, Azinhaga Sta. Comba, Celas, Coimbra 3000-548, Portugal.
e-mail: cunhavaz@aibili.pt

Received: August 19, 2025
Accepted: December 3, 2025
Published: January 22, 2026

Keywords: diabetic retinopathy; OCTA; capillary nonperfusion; hypoperfusion; hyperperfusion; MA turnover

Citation: Marques IP, Reste-Ferreira D, Santos T, Mendes L, Rocha AC, Bandello F, Parravano M, Mastropasqua L, Creuzot-Garcher C, Leal S, Baschiera F, Cunha-Vaz J. One-year progression of capillary nonperfusion in nonproliferative

Purpose: To evaluate the 1-year progression of retinal capillary nonperfusion in eyes with mild to severe nonproliferative diabetic retinopathy (NPDR) using noninvasive retinal imaging.

Methods: The CHART study (Clinicaltrials.gov: NCT04636307) is a multicenter, observational, longitudinal study involving five European research centers and included 202 eyes from 155 participants with type 2 diabetes and mild to severe NPDR. Participants underwent comprehensive ophthalmologic examinations at baseline and 3, 6, and 12 months, including best-corrected visual acuity, color fundus photography (Early Treatment Diabetic Retinopathy Study [ETDRS] severity scale), optical coherence tomography (OCT), and OCT angiography (OCTA). Disease progression was evaluated using mixed-effects models.

Results: Of the 202 eyes, 81 eyes were graded as ETDRS level 35, 63 eyes as level 43, 46 eyes as level 47, and 12 eyes as level 53. At baseline, significant differences were observed in OCTA metrics between diabetic retinopathy severity groups. A total of 169 eyes (84%) completed the 1-year follow-up. Over 1 year, eyes with ETDRS levels 35 and 43 showed significant increases in capillary nonperfusion, identified by decreases in skeletonized vessel density in the superficial capillary plexus (rates of progression: $\beta = -0.217$ mm^{-1}/y, $P = 0.006$ and $\beta = -0.310$ mm^{-1}/y, $P = 0.002$, respectively). Eyes with level 47 showed only a borderline statistically significant decrease ($P = 0.074$), while eyes with level 53 remained stable. Microaneurysm turnover (MAT), formation, and disappearance rates increased in more severe NPDR stages (levels 47 and 53).

Conclusions: Retinal capillary nonperfusion progresses significantly over 1 year in mild to moderate NPDR, identified by changes in rates of progression of vessel and perfusion densities. In more severe stages (levels 47 and 53), capillary nonperfusion stabilizes, and

diabetic retinopathy using noninvasive imaging: The CHART Study. Transl Vis Sci Technol. 2026;15(1):26, https://doi.org/10.1167/tvst.15.1.26

a hyperperfusion response is identified by increases in MAT associated with the development of intraretinal microvascular abnormalities.

Translational Relevance: This study provides quantitative data on 1-year progression of retinal capillary nonperfusion in NPDR using noninvasive imaging, offering the basis for future interventional trials.

Introduction

Diabetic retinopathy (DR) is a complication of diabetes mellitus and a leading cause of blindness worldwide, affecting approximately one-third of people living with diabetes. According to the 11th edition of the *IDF Atlas* from the International Diabetes Federation (2025), 589 million adults aged 20 to 79 years are living with diabetes globally, and by 2050, there will be 853 million people worldwide with diabetes.[1]

DR is characterized by retinal vascular abnormalities and neurodegeneration, progressing from mild nonproliferative diabetic retinopathy (NPDR) to moderate and severe NPDR and vision-threatening complications, such as proliferative diabetic retinopathy (PDR) and clinically significant macular edema (CSME).[2] Both CSME and PDR conditions may impair visual acuity, and their early detection with timely treatment is crucial to prevent vision loss.[3]

It is of great interest to be able to follow and monitor NPDR progression and to identify the parameters that characterize the progression of diabetic retinal disease, particularly using noninvasive imaging modalities. Optical coherence tomography (OCT) provides information on retinal structure and retinal segmentation that allows the automatic quantification of the macular ganglion cell layer plus inner plexiform layer (GCL + IPL) thickness, indicating neurodegeneration.[4] OCT angiography (OCTA) provides noninvasive three-dimensional mapping of capillaries in all retinal layers.[5–9] OCTA measures microvascular perfusion, offering unique insights into early retinal vascular changes and microvascular disease progression.

Additionally, microaneurysm (MA) counting and turnover performed on color fundus photographs (CFP) have been shown to be associated with NPDR progression and development of intraretinal microvascular abnormalities (IRMAs).[10–12] Identifying structural and vascular biomarkers of the different stages of disease progression is crucial for a better understanding of DR natural progression and for developing new therapeutic strategies.

In this study, we present the results of capillary nonperfusion progression during the first year of a follow-up study to characterize retinal structural and microvascular changes occurring in individuals with type 2 diabetes mellitus (T2DM) and mild to severe NPDR, using noninvasive imaging such as seven-field CFP, OCT, and OCTA at baseline and 3, 6, and 12 months.

Methods

The CHART study (Clinicaltrials.gov Identifier: NCT04636307) is a multicenter, multinational, observational, and prospective longitudinal study with a 2-year follow-up period. The study involves five European clinical research centers from three European countries (Portugal, Italy, and France), under the scientific coordination of the European Vision Institute Clinical Research Network (EVICR.net).

The clinical study was implemented and performed in accordance with the International Conference on Harmonization–Good Clinical Practice (ICH-GCP) guidelines and adheres to the tenets of the Declaration of Helsinki. Ethical approval was obtained from all relevant committees: Association for Innovation and Biomedical Research on Light and Image (AIBILI) Ethics Committee, Comité de Protection des Personnes Est IV, Comitato Etico Centrale I.R.C.C.S. Lazio Sezione IFO—Fondazione Bietti, Comitato Etico Ospedale San Raffaele, and Comitato Etico delle Province di Chieti e Pescara. Written informed consent was obtained from all participants before study enrollment and screening.

Eligibility Criteria

Inclusion criteria were the following: participants diagnosed with T2DM according to the 1985 World Health Organization definition; adults aged 35 to 90 years with NPDR level 35, 43, 47, or 53 (Early Treatment Diabetic Retinopathy Study [ETDRS] protocol based on seven-field CFP); and a spherical equivalent refraction less than 5 diopters (D).

Exclusion criteria: participants were excluded if they had hemoglobin A1C (HbA1C) levels >10% at the first visit, the presence of cataract or other

eye diseases that could interfere with fundus examinations, age-related macular degeneration, advanced glaucoma, vitreomacular disease, or other retinal vascular diseases that could affect retinopathy or visual acuity. Additional exclusions included any eye surgery within the past 6 months, previous laser treatment or intravitreal injections, comorbidities likely to affect the eye unrelated to diabetes, presence of center-involved macular edema with vision loss or requiring immediate treatment, inadequate pupil dilation (<5 mm), or uncontrolled systemic hypertension (systolic: <70 or >210 mm Hg and diastolic: <50 or >120 mm Hg). Both eyes were considered if they met all inclusion and no exclusion criteria.

Study Population

Between September 2021 and March 2023 (screening/baseline visit), 236 eyes were screened, and 202 eyes with mild to severe NPDR from 155 participants with T2DM were enrolled based on the inclusion and exclusion criteria.

This multinational study was conducted in five centers within EVICR.net in three European countries: Portugal (CS001: Centre for Clinical Trials, AIBILI, Coimbra), France (CS042: Department of Ophthalmology, University Hospital, CHU Dijon, Dijon), and Italy (CS020: IRCCS Fondazione G.B. Bietti, Rome; CS063: Excellence Eye Research Centre, University G. d'Annunzio of Chieti-Pescara, Chieti, and CS067: Department of Ophthalmology, University Vita Salute—Scientific Institute of San Raffael, Milan).

This article presents the initial 1-year progression analysis of participants followed over a 1-year period (September 2021–June 2024) with four scheduled visits: baseline, 3 months, 6 months, and 12 months or until development of vision-threatening complications (CSME/PDR). Baseline demographic and systemic data were collected, including age, sex, race, diabetes duration, comorbidities and medications, body mass index, blood pressure (systolic and diastolic), heart rate, HbA1c levels, and lipids (total cholesterol, high-density lipoprotein, low-density lipoprotein, and triglycerides).

All participants underwent comprehensive ophthalmologic examinations, including slit-lamp biomicroscopy, best-corrected visual acuity (BCVA) evaluation, intraocular pressure (IOP) measurement, and fundus imaging. DR severity was graded based on a standard seven-field CFP. OCTA images were acquired using two Zeiss (Dublin, CA, USA) devices (swept-source OCTA [SS-OCTA] and spectral-domain OCTA [SD-OCTA], using different acquisition protocols for analysis).

ETDRS-DRSS Classification

DR severity was graded using the ETDRS DR Severity Scale (DRSS) at baseline and annual visits, based on 35° seven-field CFP images acquired with retinal cameras. To ensure high-quality images, adequate dilation of the pupil of at least 5 mm was ensured using topical mydriasis (0.5% tropicamide and 0.5% phenylephrine hydrochloride).[2]

Retinal photographs were evaluated by two certified graders (IPM and ACR) at the AIBLI—Coimbra Ophthalmology Reading Centre (CORC) and classified according to the ETDRS-DRSS protocol. The ETDRS-DRSS classifications were as follows: mild NPDR (ETDRS level 35), moderate NPDR (ETDRS level 43), moderately severe NPDR (ETDRS level 47), and severe NPDR (ETDRS level 53). Changes in DR severity between baseline and the 1-year follow-up were expressed as ETDRS step changes. Eyes were categorized as stable (no change in ETDRS level), improved (one- to two-step decrease in ETDRS level), or worsened (one step or more increase in ETDRS level).

Best-Corrected Visual Acuity

BCVA was evaluated at a 4-m distance using the ETDRS protocol.[13] BCVA letter score was calculated by adding the number of letters read at 4 m plus the 30 letters read at 1 m. A change of ±5 ETDRS letters is considered a minimal clinically important difference, while a change of ≥15 letters is defined as a clinically significant gain or loss in visual acuity.

Structural Spectral-Domain OCT

Central retinal thickness (CRT) in the central subfield (retinal thickness within the 500-µm radius circle centered at the fovea) and average GCL + IPL thickness (layer thickness within the 0.5- to 2-mm radius centered at the fovea) were measured on structural data from spectral-domain OCT. Images were acquired using the Macular Cube 512 × 128 (128 B-scans with 512 A-scans each) acquisition protocol available on the Cirrus Zeiss 5000 AngioPlex (Carl Zeiss Meditec, Dublin, CA, USA).

Detailed acquisition protocols were put in place to assist technicians in consistently capturing high-quality images. Technicians were encouraged to utilize device-integrated features, such as signal strength optimization and image tracking, to enhance image quality. To further improve image quality, patients underwent pupil dilation prior to imaging, were instructed to blink, and received artificial tear instillation between image captures to maintain corneal surface hydration.

Spectral-Domain OCTA

All participants were imaged with the Cirrus Zeiss 5000 AngioPlex SD-OCTA device (Carl Zeiss Meditec) using the Angiography 3 × 3 mm (245 clusters of four B-scan repetitions with 245 A-scans) and Angiography 6 × 6 mm (350 clusters of two B-scan repetitions with 350 A-scans) acquisition protocols.

Acquisition data were exported from the ophthalmologic device and processed through the Carl Zeiss Meditec Density Exerciser (version: 10.0.12787; Carl Zeiss Meditec) to compute slab images and numerical data for the foveal avascular zone (FAZ) parameters, the skeletonized vessel density (SVD), and perfusion density (PD) metrics detected at the superficial capillary plexus (SCP). PD metrics and related images are the result of the binarization of the enface angiography images and represent changes in vessel perfusion. The skeletonization of the binary images generates SVD metrics and related images to represent the number of individual capillaries that are carrying red blood cells. Decreases in SVD and PD indicate retinal capillary nonperfusion.[14,15]

SVD and PD were measured in the inner ring (InR, 0.5- to 1.5-mm radius ring centered at the fovea) and outer ring (OutR, 1.5- to 3.0-mm radius ring centered at the fovea).

Swept-Source OCTA

Images from participants were acquired using the Angio 6 × 6 mm and Angio 15 × 15 mm acquisition protocols available in the PLEX Elite 9000 (Zeiss). This swept-source OCTA operates a tunable 1060-nm laser to provide an axial resolution of 6.3 µm. The Angio 6 × 6 mm acquisition protocol is able to scan 20° of the retina and provides angiography slab images based on two repetitions of 500 B-scans with 500 A-scans, with an acquisition rate of 100,000 A-scans/second. Furthermore, the Angio 15 × 15 mm acquisition protocol is able to scan 50° of the retina and provides angiography slab images based on two repetitions of 834 B-scans with 834 A-scans with an acquisition rate of 100,000 A-scans/second. Although with a lower axial resolution than the SD-OCTA, this device provides a wider field of view and increased definition of the deep capillary plexus (DCP) due to higher penetration of the laser source.[16–18]

Acquired data from this device were then processed using the "Macular Density v0.7.3.3" analysis protocol available on the Advanced Retina Imaging Network Hub (https://arinetworkhub.com). This analysis algorithm provides slab images for the SCP slabs and SVD and PD numerical data, similar to the one reported for the SD-OCTA device.[19] SVD and PD were measured in the InR (0.5- to 1.5-mm radius), OutR (1.5- to 3.0-mm radius), and posterior pole area (Ext1, 3- to 4.5-mm radius ring centered at the fovea; Ext2, 4.5- to 6-mm radius ring centered at the fovea; Ext3, 6- to 7.5-mm radius ring centered at the fovea).

Evaluation of OCTA Quality Images

All OCT and OCTA examinations were submitted to the AIBILI-CORC and reviewed by two certified graders, blinded to the patients' clinical status, for quality assessment. For SD-OCTA, graders reviewed each inner and outer ring quadrants for the SCP to ensure reliable metrics. If more than one quadrant was classified as low quality, the corresponding ring measurements for that slab were discarded. FAZ measurements were manually delineated on SD-OCTA 3 × 3 mm scans when image quality was poor. For SS-OCTA, vascular metrics were considered reliable if no defocus or other artifacts were absent in more than 80% of the image.

A total of 8 SD-OCTA 3 × 3 mm images (8/202; 4%) and 41 SS-OCTA 15 × 15 mm images (41/202; 20%) were excluded due to artifacts or poor signal quality.

Microaneurysm Assessment

Microaneurysm identification was automatically performed on CFP images (50°, field 2) using the RetmarkerDR (Retmarker SA, Meteda Group, Rome, Italy), a computer-aided diagnostic software certified as a class IIA medical device in Europe. The software detects red dot–like vascular lesions,[10,11] computing the number and localization of MAs in each visit, as well as the number of MAs that appear and disappear from one visit to the other, allowing the calculation of the MA disappearance and MA formation rates.[10,11] Microaneurysm turnover (MAT) is computed as the sum of the MA formation and MA disappearance rates. In this study, MA rates were calculated between baseline and 6-month visits.

Statistical Analysis

Statistical analyses were performed using STATA software version 16.1 (StataCorp LLC, College Station, Texas, USA) and R Statistical Software version 4.4.1 (R Core Team, Vienna, Austria). A P value less than 0.05 was considered statistically significant.

Data normality was assessed using the Kolmogorov–Smirnov test. Descriptive statistics

summarized demographic, systemic, and ocular parameters, as well as the distribution of diabetic retinopathy severity levels. Continuous variables were presented as means with standard deviations (SDs), medians with interquartile ranges, and minimum–maximum values. Categorical variables were reported as absolute values and percentages. Intereye agreement was assessed using intraclass correlation coefficients (ICCs).

Baseline Cross-Sectional Analysis

The primary objective of this analysis was to evaluate the baseline characteristics among different ETDRS severity groups (35, 43, 47, and 53). Linear mixed-effects models were used to account for the correlation between eyes from the same patient. Models included the differences in BCVA, IOP, OCT, and OCTA parameters, as well as MA counts with ETDRS groups (35, 43, 47, and 53), as categorical fixed-effect variables. Participants and eyes were used as nested random effects. Correlations between functional (e.g., BCVA), structural (e.g., CRT and GCL + IPL thickness), and microvascular parameters (e.g., FAZ, SVD, and PD) were assessed using Spearman's rank correlation coefficient (ρ) and interpreted as very weak ($0.00 < \rho < 0.19$), weak ($0.20 < \rho < 0.39$), moderate ($0.40 < \rho < 0.59$), strong ($0.60 < \rho < 0.79$), or very strong ($0.80 < \rho < 1.00$).[20]

Longitudinal Analysis of OCTA Progression

Subsequently, the secondary objective was to evaluate the rates of progression in OCTA parameters over a 1-year period using linear mixed-effects models for repeated measures. For this longitudinal analysis, models included changes in OCTA parameters. The categorical covariates of ETDRS levels (35, 43, 47, and 53), visit (V1M0, V2M3, V3M6, and V4M12), and their interaction (group × visit) were included as fixed effects. Participants and eyes were used as nested random effects (intercept only). Missing data were imputed implicitly by the mixed model for repeated measures.

The model provided slopes (β estimates), representing average change over time, and the confidence interval was reported for the adjusted mean for each ETDRS group and for the difference between groups. The efficacy analyses were tested at a significance level of 0.05, and all confidence intervals were two-sided at the 95% level. Positive slopes indicate an increasing trend, while negative slopes indicate a decreasing trend. Sensitivity analyses were conducted adjusting clinical sites (CS001, CS042, CS020, CS063, and CS067). Additionally, linear mixed-effects models were used to evaluate OCTA changes based on stepwise DR progression grouped as improved, stable, or worsened.

Repeatability and Reproducibility

Repeatability and reproducibility were assessed using ICCs based on images acquired on the same day for each OCTA device. Spearman's rank correlation coefficients (ρ) were also performed to assess the correlation between OCTA acquisitions from different scan sizes: SD-OCTA Angioplex (3 × 3 mm vs. 6 × 6 mm) and SS-OCTA PLEX Elite variables (6 × 6 mm vs. 15 × 15 mm), interpreted as described above.

Outcome-Based Comparisons

Mixed-effects models were also used to compare OCTA and MA parameters between participants who developed CSME/PDR and those who did not, adjusting for intereye correlation.

Results

Baseline Characteristics

The CHART study included 202 eyes from 155 participants with T2DM and mild to severe NPDR (ETDRS levels 35, 43, 47, and 53). Among them, 56 participants contributed only the right eye, 52 contributed only the left eye, and 47 contributed both eyes (94 eyes total). The mean age was 67.34 ± 9.00 years (range, 36–85 years), and 119 (77%) participants were male. Participants had a mean diabetes duration of 20.16 ± 9.51 years and a mean HbA1C level of 7.48% ± 1.10%.

The distribution of the 202 eyes across DR severity levels at baseline, based on the ETDRS classification, was as follows: 81 eyes (40%) were classified as ETDRS level 35, 63 eyes (31%) as ETDRS level 43, 46 eyes (23%) as ETDRS level 47, and 12 eyes (6%) as ETDRS level 53. Baseline demographic, systemic characteristics, and diabetic retinopathy severity of included eyes are summarized in Table 1.

Comparisons of baseline ophthalmologic examinations between different stages of NPDR are reported in Table 2 and Figure 1. Both SD-OCTA (3 × 3 mm and 6 × 6 mm) and SS-OCTA (6 × 6 mm and 15 × 15 mm) showed significant microvascular differences between mild and severe stages of DR. SVD and PD in the SCP decreased progressively with an increasing ETDRS level, reflecting increased capillary nonperfusion. Specifically, in SS-OCTA 15 × 15 mm (Fig. 2), significant differences were found between ETDRS levels 35 and 43 (SVD–ExtR3–SCP:

Table 1. Baseline Demographic Characteristics of the Participants and Diabetic Retinopathy Severity of Included Eyes

Characteristic ($n = 155$ Participants With T2DM)	Value
Participants, *n*	155
Eyes, *n*	202
Eye distribution	
Right eye	56 (28)
Left eye	52 (26)
Both eyes (right and left)	47 (46)
Sex	
Male	119 (77)
Female	36 (23)
Race	
White/Caucasian	152 (98)
African	3 (2)
Age, y	
Mean (SD)	67.34 (9.00)
Median (IQR) [Minimum–Maximum]	68.00 (14.00) [36.00–85.00]
Diabetes duration, y	
Mean (SD)	20.16 (9.51)
Median (IQR) [Minimum–Maximum]	20.00 (12.00) [1.00–48.00]
Body mass index, kg/m^2	
Mean (SD)	29.32 (4.41)
Median (IQR) [Minimum–Maximum]	28.70 (4.80) [21.10–48.40]
HbA1c, %	
Mean (SD)	7.48 (1.10)
Median (IQR) [Minimum–Maximum]	7.30 (1.40) [4.80–11.10]
Diabetic retinopathy severity levels ($n = 202$ eyes with mild to severe NPDR)	
ETDRS level 35—mild NPDR	81 (40)
ETDRS level 43—moderate NPDR	63 (31)
ETDRS level 47—moderately severe NPDR	46 (23)
ETDRS level 53—severe NPDR	12 (6)

ETDRS, Early Treatment of Diabetic Retinopathy Study; HbA1c, glycated hemoglobin; IQR, interquartile range; NPDR, nonproliferative diabetic retinopathy; SD, standard deviation.

Summary of descriptive clinical and ophthalmologic variables. Values are presented as number (%) unless otherwise indicated.

$P = 0.045$), between ETDRS levels 35 and 53 (SVD–ExtR3–SCP: $P = 0.016$ and PD–ExtR3–SCP: $P = 0.022$), and between ETDRS levels 47 and 53 (SVD–ExtR1–SCP: $P = 0.039$ and PD–ExtR1–SCP: $P = 0.024$). Overall, PD followed a similar trend as SVD measurements.

No significant baseline differences were observed between ETDRS severity groups for BCVA, IOP, CRT, and GCL + IPL thickness. However, weak but statistically significant positive correlations were found between BCVA and GCL + IPL thickness ($\rho = 0.269$, $P < 0.001$) and FAZ circularity ($\rho = 0.151$, $P = 0.038$), suggesting that decreases in GCL + IPL thickness or FAZ circularity are associated with worse BCVA.

Longitudinal Progression—1-Year Follow-up

Of the 202 enrolled eyes, 169 (84%) from 131 participants with T2DM completed the 1-year follow-up, which included visits at baseline, 3 months, 6 months, and 12 months. During this period, nine eyes (4.5%) from nine participants developed vision-threatening complications (four eyes with CSME and five eyes with PDR). One eye reached these endpoints at the 1-year visit, while the remaining eyes discontinued further follow-up after developing complications. Fifteen eyes (7.4%) from 13 participants were discontinued from the study: 13 eyes from 11 participants withdrew consent, and 2 eyes from 2 participants were lost to follow-up. Additionally, 10 eyes

Table 2. Baseline Ophthalmologic Examination by ETDRS Severity Levels

Characterisic	ETDRS Level 35 ($n = 81$)	ETDRS Level 43 ($n = 63$)	ETDRS Level 47 ($n = 46$)	ETDRS Level 53 ($n = 12$)	*P* Value (35 vs. 43)	*P* Value (43 vs. 47)	*P* Value (47 vs. 53)
Functional and ophthalmic variables							
BCVA (letters)							
Mean (SD)	82.31 (6.93)	82.46 (6.37)	83.02 (5.19)	84.25 (5.96)			
Median (IQR)	84.00 (5.00)	84.00 (6.00)	85.00 (5.00)	85.00 (7.50)	0.531	0.991	0.265
IOP (mm Hg)							
Mean (SD)	15.78 (3.14)	16.35 (2.95)	16.04 (3.45)	17.58 (4.66)			
Median (IQR)	15.00 (4.00)	16.00 (4.00)	15.50 (5.00)	18.00 (8.50)	0.856	0.923	0.169
Structural SD-OCT							
CRT—average CSF (µm)							
Mean (SD)	265.51 (24.71)	271.11 (23.34)	273.18 (26.88)	273.42 (21.62)			
Median (IQR)	265.00 (34.00)	273.00 (33.00)	272.00 (29.00)	273.50 (30.50)	0.222	0.649	0.948
GCL + IPL thickness (µm)							
Mean (SD)	76.80 (9.91)	79.78 (10.28)	77.89 (10.29)	71.92 (16.42)			
Median (IQR)	78.00 (11.00)	77.00 (12.00)	79.00 (9.00)	75.00 (26.00)	0.320	0.777	0.167
SS-OCTA PLEX Elite (15 × 15 mm)							
FAZ area (mm^2)							
Mean (SD)	0.35 (0.09)	0.34 (0.14)	0.36 (0.10)	0.37 (0.06)			
Median (IQR)	0.35 (0.12)	0.31 (0.15)	0.31 (0.15)	0.39 (0.04)	0.948	0.775	0.407
SVD–InR–SCP (mm^{-1})							
Mean (SD)	15.12 (2.27)	14.43 (2.39)	15.05 (2.00)	14.51 (2.01)			
Median (IQR)	15.44 (2.92)	14.66 (3.46)	15.28 (2.20)	14.24 (3.74)	0.154	0.203	0.349
SVD–OutR–SCP (mm^{-1})							
Mean (SD)	15.68 (1.89)	15.50 (1.71)	15.99 (1.59)	14.57 (2.25)			
Median (IQR)	16.02 (2.69)	15.85 (2.38)	15.99 (2.42)	15.19 (1.94)	0.630	0.211	0.054
SVD–ExtR1– SCP (mm^{-1})							
Mean (SD)	15.29 (1.80)	15.45 (1.29)	15.71 (1.28)	14.35 (2.03)			
Median (IQR)	15.59 (2.63)	15.60 (1.68)	15.81 (1.54)	14.53 (1.78)	0.646	0.461	0.039*
SVD–ExtR2– SCP (mm^{-1})							
Mean (SD)	13.30 (1.61)	13.12 (1.42)	13.27 (1.38)	12.18 (1.74)			
Median (IQR)	13.31 (2.59)	13.16 (2.25)	13.50 (1.98)	12.42 (2.04)	0.555	0.565	0.073
SVD–ExtR3– SCP (mm^{-1})							
Mean (SD)	11.04 (1.96)	10.39 (1.79)	10.55 (1.78)	9.73 (1.52)			
Median (IQR)	11.52 (3.10)	10.48 (2.91)	10.60 (2.41)	9.68 (1.75)	0.045*	0.441	0.094

BCVA, best corrected visual acuity; CRT, central retinal thickness; CSF, central subfield; ExtR, extended ring; FAZ, foveal avascular zone; GCL+IPL, ganglion cell layer plus inner plexiform layer; InR, inner ring; IOP, intraocular pressure; OutR, outer ring; SCP, superficial capillary plexus; SD-OCT, spectral domain optical coherence tomography; SS-OCTA, swept-source optical coherence tomography angiography; SVD, skeletonized vessel density.

Perfusion density (PD) parameters followed trends similar to skeletonized vessel density measurements. Detailed PD data are not presented in the main tables for brevity.

*Statistically significant differences with $P < 0.05$ using linear mixed-effect models, taking into account correlated eye data.

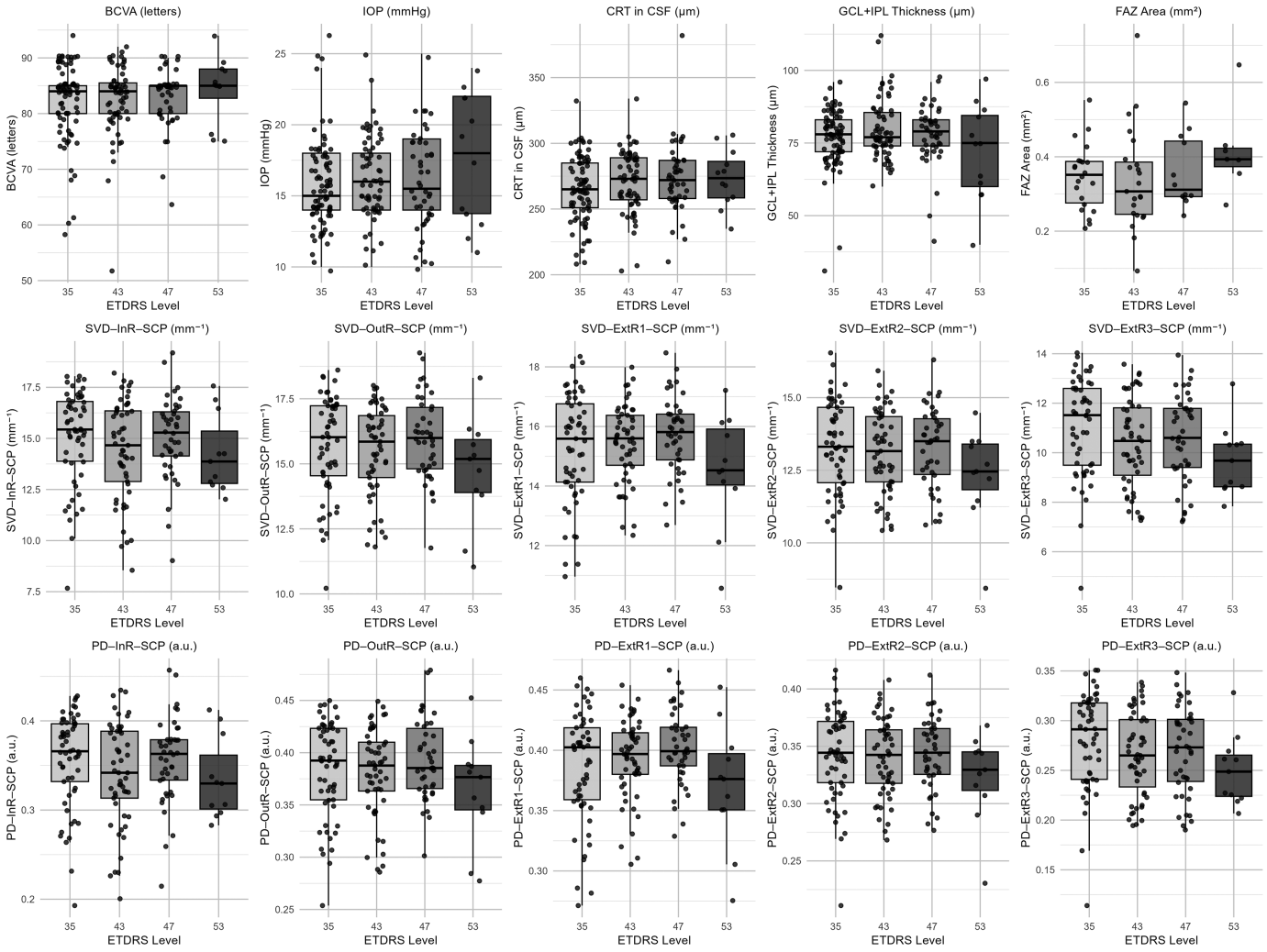

Figure 1. Baseline comparison between ETDRS severity levels.

missed scheduled visits due to health-related issues or incapacity.

Of the 169 eyes that completed the 1-year follow-up, baseline DR severity was distributed as follows: 78 eyes (46%) were classified as ETDRS level 35, 57 eyes (34%) as level 43, 29 eyes (17%) as level 47, and 5 eyes (3%) as level 53. These eyes were included in the longitudinal analysis to evaluate disease progression at baseline, 3 months, 6 months, and 12 months.

Significant longitudinal changes were observed for both SD-OCTA (3 × 3 mm and 6 × 6 mm) and SS-OCTA (6 × 6 mm and 15 × 15 mm) (Table 3; Fig. 3). In SD-OCTA 3 × 3 mm, eyes classified as ETDRS level 43 showed significant annual changes in FAZ metrics. Specifically, both FAZ area and perimeter increased significantly ($\beta = 0.006$ mm^2/y with $P = 0.014$ and $\beta = 0.059$ mm/y with $P = 0.013$, respectively), while FAZ circularity decreased significantly ($\beta = -0.014$ a.u./y with $P = 0.005$). In addition, a significant decrease in SVD in the SCP at the inner ring was observed in eyes with ETDRS levels 35 ($\beta = -0.153$ mm^{-1}/y with $P = 0.008$), 43 ($\beta = -0.208$ mm^{-1}/y with $P = 0.004$), and 47 ($\beta = -0.241$ mm^{-1}/y with $P = 0.005$). In contrast, eyes with ETDRS level 53 showed stabilization over the 1-year period. However, pairwise comparisons between ETDRS levels ($\Delta\beta$) did not reach statistical significance.

Similarly, the SS-OCTA 6 × 6 mm and 15 × 15 mm acquisition protocols showed similar trends in microvascular changes over 1 year. In the SS-OCTA with 15 × 15 mm, eyes with ETDRS levels 35 and 43 showed a significant decrease in SVD in the SCP at the OutR ($\beta = -0.217$ mm^{-1}/y with $P = 0.006$ and $\beta = -0.310$ mm^{-1}/y with $P = 0.002$, respectively). Eyes with level 47 showed a borderline significant decrease (OutR: $\beta = -0.165$ mm^{-1}/y, $P = 0.074$ and ExtR1: -0.297 mm^{-1}/y, $P = 0.001$), while eyes with ETDRS level 53 showed stabilization of the perfu-

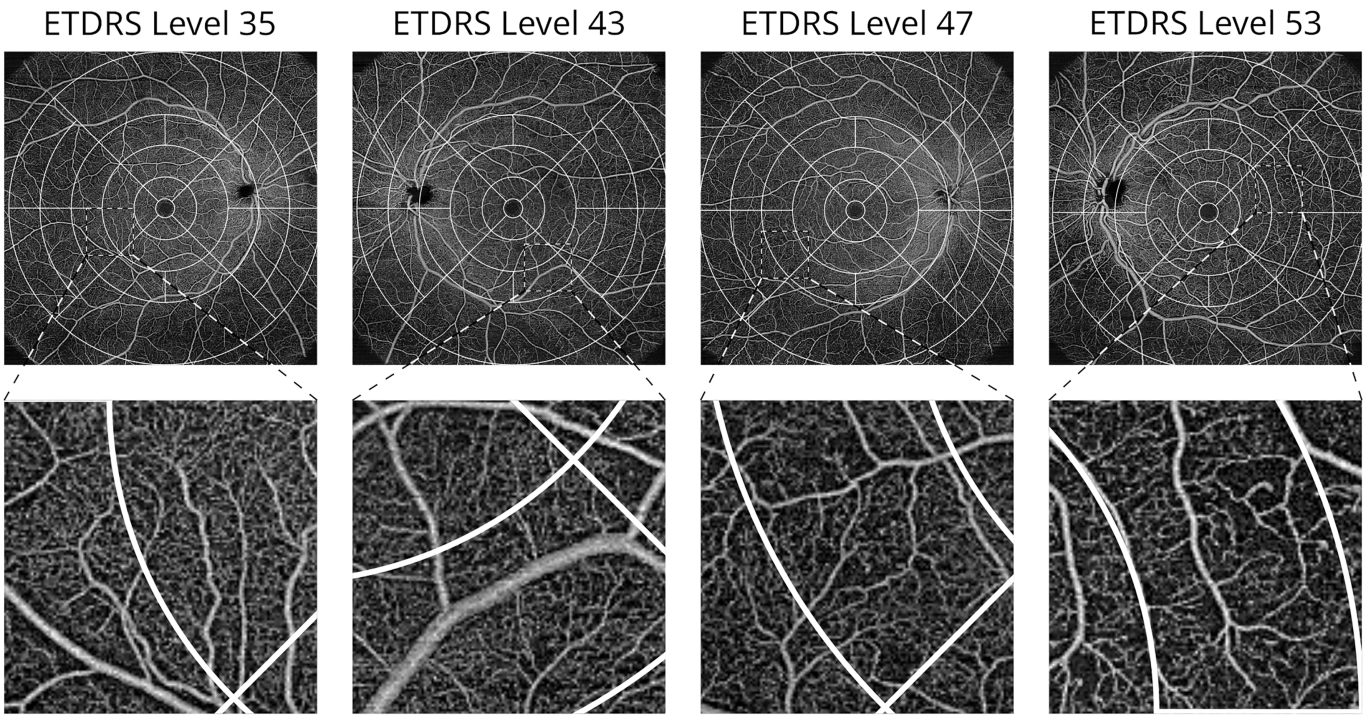

Figure 2. OCTA by ETDRS severity levels.

sion metrics. Among all groups, eyes with ETDRS level 43 showed the most pronounced progression rate, but pairwise comparisons between ETDRS levels ($\Delta\beta$) did not reach statistical significance. Consistent patterns of progression were also observed in the DCP, extended rings, and PD metrics. Statistically significant mean differences were observed only between ETDRS levels 43 and 53 (SVD–ExtR2–SCP: $\Delta\beta = 0.498\ \text{mm}^{-1}/\text{y}$ with $P = 0.018$ and SVD–ExtR3–SCP: $\Delta\beta = 0\ .574\ \text{mm}^{-1}/\text{y}$ with $P = 0.033$).

Multicenter Study

This multicenter and multinational study was conducted across five clinical centers in three European countries (Portugal, Italy, and France). Despite observable intersite variability in the different imaging protocols, the longitudinal decreases in SVD and PD remained statistically significant after adjusting for intersite variability, underscoring the robustness of the findings and demonstrating that use of OCTA metrics for retinal nonperfusion quantification is feasible in a multicenter study.

For example, after adjustment, SVD in the SCP outer ring (SS-OCTA 15 × 15 mm) varied from $\beta = -0.217$ to $\beta = -0.341\ \text{mm}^{-1}/\text{y}$ ($P = 0.007$) in ETDRS level 35 and from $\beta = -0.310$ to $\beta = -0.580\ \text{mm}^{-1}/\text{y}$ ($P = 0.001$) in ETDRS level 43, whereas ETDRS levels 47 and 53 showed stabilization.

Variability in OCTA Devices and Scan Protocols

All OCTA devices (SD-OCTA and SS-OCTA) were available at all clinical sites, and imaging was evaluated and performed at all scheduled time points. OCTA measurements differed based on the device (SD-OCTA vs. SS-OCTA), scan protocols (3 × 3 mm vs. 6 × 6 mm vs. 15 × 15 mm), and the metrics assessed (e.g., SVD and PD). Despite these differences, retinal nonperfusion metrics showed good to excellent repeatability based on ICCs, derived from same-day image acquisitions for each OCTA device. For example, SVD at the InR in the SCP showed the highest repeatability with SD-OCTA 3 × 3 mm scans (ICC = 0.847), followed by SD-OCTA 6 × 6 mm and SS-OCTA 15 × 15 mm (ICC = 0.792 and 0.787, respectively). Lower repeatability was observed with SS-OCTA 6 × 6 mm (ICC = 0.741).

In addition, Spearman correlation analyses showed moderate to strong associations across different OCTA devices and protocols. For example, for SVD at the InR in the SCP, a strong correlation was found between the SD-OCTA 3 × 3 mm and 6 × 6 mm scans ($\rho = 0.616$, $P < 0.001$). SS-OCTA 6 × 6 mm and 15 × 15 mm scans showed moderate correlations (OutR: $\rho = 0.464$, $P < 0.001$). A weaker but statistically significant correlation was noted between SD-OCTA 3 × 3 mm and SS-OCTA 15 × 15 mm ($\rho = 0.241$, $P = 0.002$).

Table 3. Longitudinal Changes for SD-OCTA Angioplex 3 × 3 mm and SS-OCTA PLEX Elite 15 × 15 mm

Parameter	Time Point	ETDRS Level 35 ($n = 78$)	ETDRS Level 43 ($n = 57$)	ETDRS Level 47 ($n = 29$)	ETDRS Level 53 ($n = 5$)
SD-OCTA Angioplex 3 × 3 mm					
FAZ area (mm^2)	0M (Mean ± SD)	0.28 ± 0.10	0.29 ± 0.11	0.30 ± 0.12	0.28 ± 0.13
	3M (Mean ± SD)	0.29 ± 0.10	0.30 ± 0.10	0.31 ± 0.12	0.28 ± 0.14
	6M (Mean ± SD)	0.29 ± 0.10	0.31 ± 0.10	0.32 ± 0.13	0.32 ± 0.12
	12M (Mean ± SD)	0.29 ± 0.11	0.31 ± 0.11	0.32 ± 0.14	0.34 ± 0.10
	Slope ($\beta \pm$ SE)	0.002 ± 0.001	0.006 ± 0.002	0.002 ± 0.003	0.007 ± 0.007
	(P value)	(0.260)	(0.014)*	(0.404)	(0.279)
SVD–InR–SCP (mm^{-1})	0M (Mean ± SD)	19.03 ± 1.90	18.88 ± 1.85	19.21 ± 1.68	19.55 ± 1.60
	3M (Mean ± SD)	18.90 ± 1.99	18.63 ± 1.77	19.00 ± 1.62	19.38 ± 1.49
	6M (Mean ± SD)	18.81 ± 2.04	18.46 ± 1.79	18.78 ± 1.79	18.97 ± 1.61
	12M (Mean ± SD)	18.59 ± 1.99	18.23 ± 2.18	18.22 ± 1.49	19.46 ± 1.16
	Slope ($\beta \pm$ SE)	−0.153 ± 0.058	−0.208 ± 0.072	−0.241 ± 0.085	−0.264 ± 0.167
	(P value)	(0.008)*	(0.004)*	(0.005)*	(0.114)
SS-OCTA PLEX Elite 15 × 15 mm					
SVD–InR–SCP (mm^{-1})	0M (Mean ± SD)	15.12 ± 2.27	14.43 ± 2.39	15.05 ± 2.00	14.24 ± 1.90
	3M (Mean ± SD)	14.05 ± 2.82	14.17 ± 2.87	15.10 ± 1.76	15.02 ± 2.18
	6M (Mean ± SD)	14.71 ± 2.38	14.05 ± 2.27	14.88 ± 1.96	14.24 ± 2.49
	12M (Mean ± SD)	14.03 ± 2.34	13.06 ± 2.89	14.53 ± 2.14	15.01 ± 1.49
	Slope ($\beta \pm$ SE)	−0.289 ± 0.104	−0.406 ± 0.144	−0.070 ± 0.113	0.118 ± 0.255
	(P value)	(0.006)*	(0.005)*	(0.536)	(0.644)
SVD–OutR–SCP (mm^{-1})	0M (Mean ± SD)	15.68 ± 1.89	15.50 ± 1.71	15.99 ± 1.59	14.75 ± 2.08
	3M (Mean ± SD)	15.27 ± 2.17	15.34 ± 2.36	15.91 ± 1.61	15.57 ± 2.54
	6M (Mean ± SD)	15.52 ± 1.90	15.05 ± 1.67	15.79 ± 1.66	15.10 ± 3.25
	12M (Mean ± SD)	15.03 ± 1.99	14.46 ± 2.11	15.18 ± 1.78	15.98 ± 0.90
	Slope ($\beta \pm$ SE)	−0.217 ± 0.079	−0.310 ± 0.100	−0.165 ± 0.092	0.038 ± 0.201
	(P value)	(0.006)*	(0.002)*	(0.074)	(0.850)

Table 3. Continued

Parameter	Time Point	ETDRS Level 35 ($n = 78$)	ETDRS Level 43 ($n = 57$)	ETDRS Level 47 ($n = 29$)	ETDRS Level 53 ($n = 5$)
SVD–Ext1–SCP (mm^{-1})	0M (Mean ± SD)	15.29 ± 1.80	15.45 ± 1.29	15.71 ± 1.28	14.53 ± 1.90
	3M (Mean ± SD)	15.04 ± 1.94	15.35 ± 1.77	15.47 ± 1.44	14.92 ± 2.53
	6M (Mean ± SD)	15.22 ± 1.69	14.93 ± 1.30	15.34 ± 1.39	14.34 ± 3.18
	12M (Mean ± SD)	14.80 ± 1.85	14.34 ± 1.92	14.56 ± 1.76	15.99 ± 0.45
	Slope ($\beta \pm$ SE)	−0.185 ± 0.063	−0.333 ± 0.081	−0.297 ± 0.087	0.088 ± 0.244
	(*P* value)	(0.003)*	(<0.001)	(0.001)*	(0.717)
SVD–Ext2–SCP (mm^{-1})	0M (Mean ± SD)	13.30 ± 1.61	13.12 ± 1.42	13.27 ± 1.38	12.33 ± 1.60
	3M (Mean ± SD)	13.00 ± 1.86	12.83 ± 1.50	12.94 ± 1.35	12.95 ± 1.66
	6M (Mean ± SD)	12.94 ± 1.67	12.46 ± 1.37	13.05 ± 1.39	12.13 ± 1.42
	12M (Mean ± SD)	12.87 ± 1.89	12.09 ± 2.02	12.57 ± 1.47	13.68 ± 0.90
	Slope ($\beta \pm$ SE)	−0.170 ± 0.057	−0.311 ± 0.071	−0.194 ± 0.080	0.193 ± 0.210
	(*P* value)	(0.003)*	(<0.001)*	(0.015)*	(0.358)
SVD–Ext3–SCP (mm^{-1})	0M (Mean ± SD)	11.04 ± 1.96	10.39 ± 1.79	10.55 ± 1.78	9.70 ± 1.41
	3M (Mean ± SD)	10.51 ± 2.30	10.15 ± 1.70	10.23 ± 1.63	10.10 ± 1.91
	6M (Mean ± SD)	10.50 ± 1.64	9.79 ± 1.49	10.57 ± 1.80	10.20 ± 1.72
	12M (Mean ± SD)	10.52 ± 2.24	9.59 ± 2.36	10.01 ± 1.83	10.96 ± 1.11
	Slope ($\beta \pm$ SE)	−0.196 ± 0.080	−0.264 ± 0.085	−0.131 ± 0.105	0.318 ± 0.165
	(*P* value)	(0.014)*	(0.002)*	(0.212)	(0.053)

Ext, extended rings; M, months; N, number; SE, standard error; SVD, skeletonized vessel density.

Rates of changes in foveal avascular zone, skeletonized vessel density, and perfusion density were calculated using linear mixed-effects models. PD parameters followed trends similar to SVD measurements. Detailed PD data are not presented in the main tables for brevity The models analyzed changes in OCTA parameters from visit 1 (baseline) to visit 4 (12 months), considering the four time points (V1M0, V2M3, V3M6, and V4M12) as the response variable. Fixed effects included categorical covariates for ETDRS severity levels (35, 43, 47, and 53), visit (V1M0, V2M3, V3M6, and V4M12), and the interaction (group × visit), as fixed effects. Participants, eyes, and clinical sites were used as nested random effects (intercept only). Missing data were imputed implicitly by the mixed model for repeated measures. The slope (β) represents the adjusted mean year change within each ETDRS group over time.

*Statistical significance was tested at the 0.05 level, with all confidence intervals two-sided at the 95% confidence level. Positive slopes indicate an increasing trend while negative slopes indicate a decreasing trend.

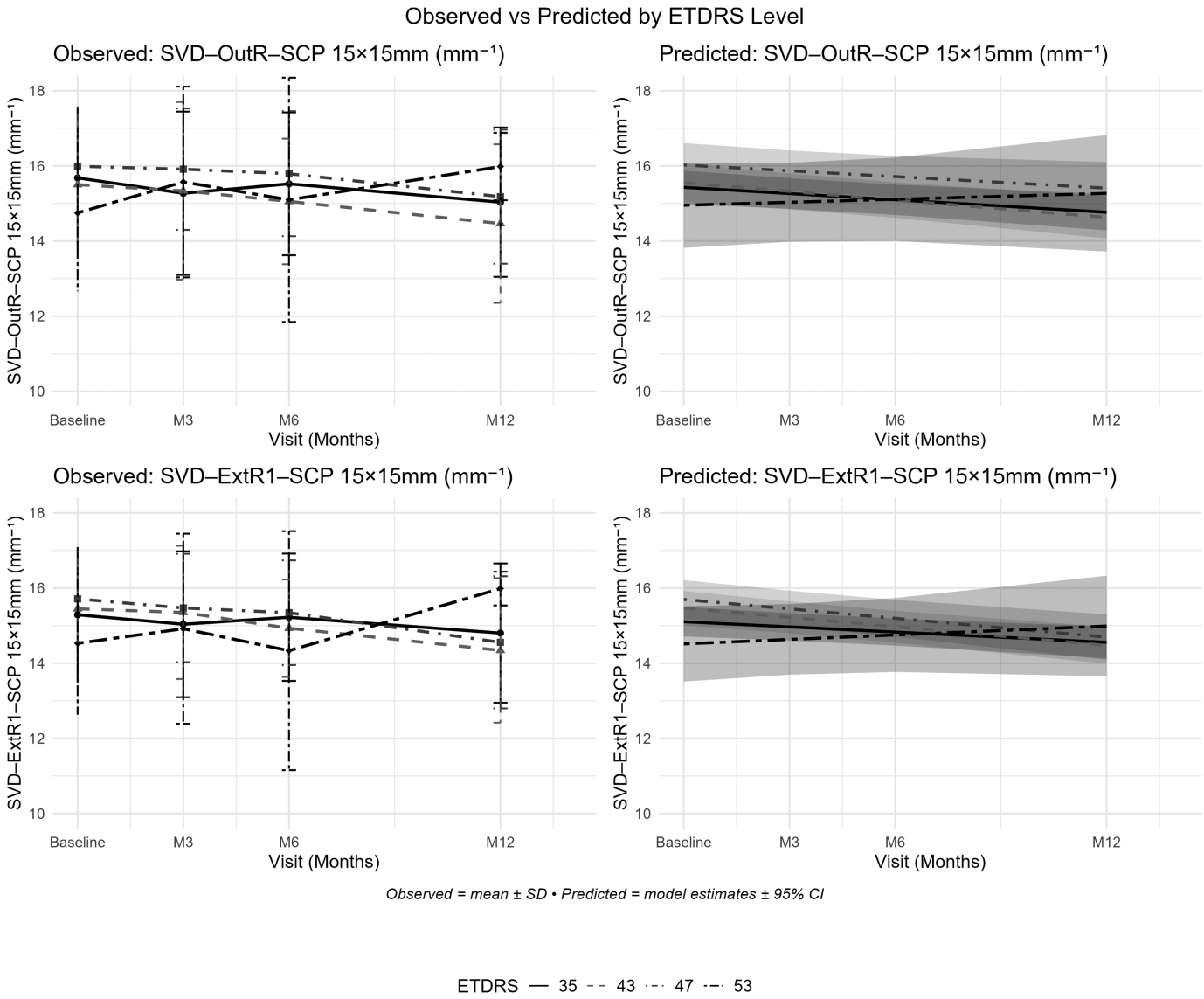

Figure 3. Rates of changes in SVD metrics in SCP over a 1-year follow-up period between the different ETDRS severity groups included in the study.

Across all imaging protocols and devices, a consistent decline in SVD in the inner ring at the SCP was observed. For example, in eyes with ETDRS level 35, the annual rates of progression were $\beta = -0.153\ \text{mm}^{-1}/\text{y}$ ($P = 0.008$) with SD-OCTA 3 × 3 mm, $\beta = -0.332\ \text{mm}^{-1}/\text{y}$ ($P < 0.001$) with SD-OCTA 6 × 6 mm, $\beta = -0.286\ \text{mm}^{-1}/\text{y}$ ($P < 0.001$) with SS-OCTA 6 × 6 mm, and $\beta = -0.289\ \text{mm}^{-1}/\text{y}$ ($P = 0.006$) with SS-OCTA 15 × 15 mm. Among these, the SD-OCTA 6 × 6 mm scan showed the steepest annual decline. Additionally, only the 3 × 3 mm scans detected a significant longitudinal increase in FAZ metrics in eyes with ETDRS level 43 (e.g., FAZ area: $\beta = 0.006\ \text{mm}^2/\text{y}$ with $P = 0.014$), highlighting their potential to capture early microvascular changes. These findings demonstrate that despite differences in scan size and OCTA technology, measuring rates of progression in microvascular changes instead of absolute values in SVD and PD allows more consistent and reliable monitoring, minimizing variability across imaging devices, protocols, and sites.

Microaneurysm Turnover and Disease Progression

Our results also show that MAT, as well as formation and disappearance rates over a 6-month period, increased with increased DR severity ($P < 0.05$). Notably, these increases were more pronounced at the advanced stages—ETDRS levels 47 and 53 (Table 4).

Table 4. Microaneurysm Assessment over a 6-Month Period

Baseline and 6 Months	ETDRS Level 35 ($n = 77$)	ETDRS Level 43 ($n = 57$)	ETDRS Level 47 ($n = 35$)	ETDRS Level 53 ($n = 7$)	*P* Value
MA formation rate					35 vs. 43: 0.017*; 35 vs. 47: <0.001*; 35 vs. 53: <0.001*; 43 vs. 47: 0.078; 43 vs. 53: <0.001*; 47 vs. 53: <0.001*
Mean (SD)	1.35 (2.02)	4.47 (6.00)	7.07 (9.16)	19.52 (25.52)	
Median (IQR)	0.00 (2.00)	2.00 (7.00)	4.25 (10.20)	10.90 (6.40)	
MA disappearance rate					35 vs. 43: 0.014*; 35 vs. 47: 0.001*; 35 vs. 53: <0.001*; 43 vs. 47: 0.257; 43 vs. 53: <0.001*; 47 vs. 53: <0.001*
Mean (SD)	1.49 (2.26)	4.89 (6.91)	5.79 (5.43)	21.24 (26.70)	
Median (IQR)	0.00 (2.10)	3.90 (6.30)	4.10 (8.60)	8.70 (8.30)	
MA turnover					35 vs. 43: 0.009*; 35 vs. 47: <0.001*; 35 vs. 53: <0.001*; 43 vs. 47: 0.095; 43 vs. 53: <0.001*; 47 vs. 53: <0.001*
Mean (SD)	2.84 (3.49)	9.36 (10.91)	12.86 (12.51)	40.76 (52.07)	
Median (IQR)	2.00 (4.30)	6.30 (11.80)	10.05 (15.00)	17.50 (14.70)	

*Statistically significant differences with $P < 0.05$ using linear mixed-effect models. MA rates were calculated using baseline and 6-month follow-up visits.

Table 5. Six-Month OCTA and Microaneurysm Progression Rates by Clinical Outcome

Baseline and 6-Month Rates of Progression in OCTA and MA	No Outcome ($n = 160$)	Outcome (CSME/PDR) ($n = 9$[a])	Mean Change (SE) [95% CI]	*P* Value
SVD–InR–SCP			−2.39 ± 1.76 [−5.84 to 1.06]	0.174
$\beta \pm$ SE [95% CI]	−0.47 ± 0.40 [−1.26 to 0.32]	−2.67 ± 1.35 [−5.32 to −0.01]		
P value	0.246	0.049*		
SVD–OutR–SCP			−2.71 ± 1.39 [−5.45 to 0.02]	0.052
$\beta \pm$ SE [95% CI]	−0.35 ± 0.32 [−0.98 to 0.28]	−2.69 ± 1.22 [−5.07 to −0.30]		
P value	0.277	0.027*		
MA formation rate			8.80 (2.89) [3.14 to 14.45]	0.002*
Mean (SD)	3.71 (6.04)	12.74 (23.12)		
Median (IQR)	1.75 (4.40)	4.20 (9.70)		
MA disappearance rate			11.47 (2.61) [6.36 to 16.58]	<0.001*
Mean (SD)	3.56 (5.34)	15.69 (23.49)		
Median (IQR)	2.00 (5.80)	8.50 (5.40)		
MA turnover			19.75 (5.05) [9.86 to 29.64]	<0.001*
Mean (SD)	7.27 (9.85)	28.43 (46.46)		
Median (IQR)	3.90 (10.00)	10.50 (13.00)		

CI, confidence interval.

Linear mixed-effects model was applied to assess differences in SS-OCTA (15 × 15 mm) and MA parameters between participants who developed vision-threatening complications (outcome group: CSME/PDR) and those who did not (no-outcome group). Group classification (outcome versus no outcome) was included as a categorical variable, with participants and eyes as nested random effects (intercept only).

[a]Two participants eyes developed complications prior to the 6-month visit, which was used as the time point for calculating baseline and 6 months.

*The efficacy analyses were tested at a significance level of 0.05, and all confidence intervals were two-sided and at the 95% level. OCTA and MA rates were calculated between baseline and 6-month visits.

Disease Progression Based on ETDRS Severity Changes

At the 1-year follow-up (n = 169 eyes), 22 eyes (13%) progressed to more advanced stages of ETDRS, including 20 eyes with one-step worsening and 2 eyes with two-step worsening. In contrast, 118 eyes (70%) maintained the same ETDRS severity level from baseline to the 12-month visit, and 27 eyes (16%) showed improvement in ETDRS levels. Two eyes (1%) could not be classified. Worsening eyes showed a significant decrease in SVD in the SCP at the inner ring ($\beta = -0.716$ mm^{-1}/y, $P = 0.004$) compared to those that remained stable or improved ($\beta = -0.185$ mm^{-1}/y, $P = 0.017$). The difference in progression rates between these groups was statistically significant ($\Delta\beta = -0.538$ mm^{-1}/y, $P = 0.016$), indicating an association between capillary nonperfusion (SVD loss) and disease severity worsening.

Vision-Threatening Complications

During the 1-year follow-up period, vision-threatening complications were observed in nine eyes (4.5%), including four eyes showing CSME (baseline ETDRS levels 43 and 47) and five eyes developing PDR (baseline ETDRS levels 47 and 53). When analyzing 6-month OCTA progression rates by clinical outcome, significant declines in SVD were observed in the SCP at both the inner and outer rings ($\beta = -2.67$ mm^{-1}/y with $P = 0.049$ and $\beta = -2.69$ mm^{-1}/y with $P = 0.027$, respectively) among eyes with complications, whereas changes in the no-outcome group were not statistically significant (Table 5). Additionally, MA formation rate, disappearance rate, and turnover at 6 months were significantly different between eyes that developed vision-threatening complications and those that did not ($P = 0.002$, $P < 0.001$, and $P < 0.001$, respectively).

It is particularly relevant that a strong negative correlation was identified between capillary nonperfusion and MAT in these eyes with CSME and/or PDR ($\rho = -0.893$ with $P = 0.007$), indicating that an increase in MAT is associated with a decrease in SVD in the SCP.

Discussion

This multicenter, observational, and longitudinal study shows that using OCTA metrics and CFP, both noninvasive examination methods, it is possible to identify and quantify the progression of microvascular disease over a period of 1 year in participants with T2DM and mild to severe NPDR (ETDRS levels 35, 43, 47, and 53). These results were obtained from five centers across different European countries (Portugal, Italy, and France), demonstrating the feasibility of clinical trials using noninvasive OCTA and multicenter participation.

The results obtained in this study show that progression of retinal capillary nonperfusion in NPDR can be identified and quantified by using rates of progression of the SVD and PD metrics determined by noninvasive OCTA. In this study, visits at baseline, 3 months, 6 months, and 12 months were considered.[21,22]

Early NPDR stages (ETDRS levels 35 and 43) are characterized by progressive capillary nonperfusion (hypoperfusion), followed by a hyperperfusion response present in more advanced stages—ETDRS levels 47 and 53. This hyperperfusion response is characterized by an increased number of MAs, apparently associated with the development of the IRMAs.[23,24] The increased number of MAs, as well as their formation and disappearance rates, appear to be good indicators of the presence of IRMAs, as first described by Cogan and Kuwabara.[8,25] In DRCR.net Protocol AA, using ultrawidefield fluorescein angiography, Silva et al.[26] have shown that capillary nonperfusion is associated with disease progression and may serve as a marker of retinopathy worsening.

The pattern of NPDR disease progression identified in this study also corroborates the progression pattern suggested by Curtis et al.,[27] characterized by a hypoperfusion stage, followed by a hyperperfusion stage in more advanced stages of NPDR. This pattern has also been confirmed by previous work of our group.[8,28] Understanding NPDR progression appears to be achieved by assessing the balance between these two stages, particularly in the more severe stages of DR.

This multicenter study provides important evidence supporting the value of OCTA to quantify capillary nonperfusion (hypoperfusion stage) as a marker of DR progression, using SVD and PD metrics. It shows also the value of counting MA and calculating MA turnover, using CFP, to identify the hyperperfusion response.[29,30]

Another relevant finding is that the rate of progression of retinal capillary nonperfusion in ETDRS level 43 appears to be increased compared to ETDRS level 35, suggesting more rapid progression of capillary nonperfusion in this stage of disease. In contrast, stabilization of the retinal nonperfusion appears to occur in ETDRS stages 47 and 53, suggesting that the retinal capillary nonperfusion reaches a ceiling.[8,25] However, given the small number of eyes in these subgroups, these observations should be interpreted with caution. Identifying a potential ceiling of capillary nonperfu-

sion could be relevant for future therapeutic strategies, such as titrating laser therapy, but these findings need further exploration.

When analyzing progression of NPDR, it is crucial to follow closely the ETDRS classification of DR severity. Consistent with previous reports, this study shows that ETDRS severity levels 35 and 43 can be characterized by the progressive increase in capillary nonperfusion (hypoperfusion stage), followed by ETDRS severity levels 47 and 53, which are characterized by stabilization of capillary nonperfusion and rapid increase in the number of MAs, which appear to reflect the development of IRMAs. These features appear to represent potential risk markers for vision-threatening complications (CSME and PDR), but further studies in larger cohorts are needed to validate these findings.

OCTA metrics are associated with considerable variability, mostly due to different acquisition protocols and variable conditions of the eyes at the time of examination. The quantification of rates of progression in capillary nonperfusion using noninvasive OCTA in this study appears to be a more reliable approach to test the efficacy of therapeutic interventions. We show in this study that by using a minimum of two examinations, separated by an interval of 6 months to measure rates of progression in the SVD or PD, it is possible to identify progression in capillary nonperfusion. This metric appears to be less affected by individual variations.

Limitations of this study include, first, the inclusion of participants with acceptable metabolic control and the exclusion of participants with HbA1c values >10%. However, this is also a positive factor regarding the design of future trials testing potential therapies addressing retinal microvascular hypoperfusion and/or hyperperfusion. The small sample size in the ETDRS level 53 subgroup ($n = 12$, with only five eyes completing a 1-year follow-up) limits the statistical power and generalizability of the findings for this group, and these results should therefore be interpreted with caution. Capillary nonperfusion was assessed exclusively using noninvasive OCTA-derived metrics (SVD and PD), since fluorescein angiography, an invasive method, was not performed. Nevertheless, previous studies have demonstrated a correspondence between decreases in OCTA vessel densities (i.e., capillary nonperfusion) and the presence of increased ischemic index values.[8]

Differences in microvascular metrics across OCTA devices, specifically SD-OCTA versus SS-OCTA, were apparent in this study and are another relevant limitation. Variability arising from differences in device hardware, segmentation algorithms, and motion artifact susceptibility also contributes to both inter- and intrasession measurement variability.[31,32] However, the use of progression rates instead of absolute OCTA values appears to decrease the variability of the results.

Finally, these are preliminary 1-year results (baseline, 3 months, 6 months, and 12 months). Continued follow-up into year 2 will provide additional data, allowing for a more comprehensive understanding of NPDR progression using noninvasive imaging modalities.

In conclusion, the ability to monitor the balance between the capillary nonperfusion (hypoperfusion stage) and the hyperperfusion response using rates of changes of OCTA-derived SVD/PD parameters and MA counting or turnover, using CFP, both noninvasive methods, opens new perspectives and provides new opportunities to predict the risk of progression to vision-threatening complications. Our findings also demonstrate the feasibility of multicentric clinical studies using noninvasive OCTA and MA counting.

Acknowledgments

The authors thank the entire CHART Study team.

The CHART study (Clinicaltrials.gov: NCT046 36307) is an Investigator-Initiated Research (IIR) sponsored by AIBILI and funded by Bayer through an IIR grant.

Author Contributors: Inês Pereira Marques, Débora Reste-Ferreira, Torcato Santos, Luís Mendes, Ana Cláudia Rocha, Francesco Bandello, Mariacristina Parravano, Leonardo Mastropasqua, Catherine Creuzot-Garcher, Sérgio Leal, Fabio Baschiera and José Cunha-Vaz designed and conducted the experiment, analyzed and interpreted the data, wrote and revised the manuscript. José Cunha-Vaz is the guarantor of this work and, as such, had full access to all the data in the study and takes responsibility for the integrity of the data and the accuracy of the data analysis. All authors have read and agreed to the published version of the manuscript.

Ethics Approval: The CHART study (Clinicaltrials.gov identifier: NCT04636307) adheres to the tenets of the Declaration of Helsinki and follows the International Conference on Harmonization–Good Clinical Practice (ICH-GCP) guidelines. Ethical approval for the study was obtained by the respective Ethics Committees in accordance with national regulations: Association for Innovation and Biomedical Research

on Light and Image (AIBILI) Ethics Committee (CS001), Ethics Committee—Comité de Protection des Personnes Est IV (CS042), Comitato Etico Centrale I.R.C.C.S. Lazio Sezione IFO—Fondazione Bietti (CS020), Comitato Etico Ospedale San Raffaele (CS067), and Comitato Etico delle Province di Chieti e Pescara (CS063). Written informed consent to participate in the CHART clinical study was obtained from all participants prior to being screened.

Data Availability Statements: Datasets generated during and/or analyzed during the current study are available from the corresponding author on reasonable request.

Disclosure: **I.P. Marques**, None; **D. Reste-Ferreira**, None; **T. Santos**, None; **L. Mendes**, None; **A.C. Rocha**, None; **F. Bandello**, Bayer (C); **M. Parravano**, Bayer (C); **L. Mastropasqua**, Bayer (C); **C. Creuzot-Garcher**, Bayer (C); **S. Leal**, Bayer (E); **F. Baschiera**, Bayer (E); **J. Cunha-Vaz**, Bayer (C, F), Boehringer Ingelheim (C, F), Carl Zeiss Meditec (C, F), Roche (C)

References

1. International Diabetes Federation. *International Diabetes Federation. IDF Diabetes Atlas*. 11th ed. Brussels: International Diabetes Federation; 2025.
2. Early Treatment Diabetic Retinopathy Study Research Group. Grading diabetic retinopathy from stereoscopic color fundus photographs—an extension of the modified Airlie House Classification: ETDRS Report Number 10. *Ophthalmology*. 1991;98(5):786–806.
3. Cunha-Vaz J, Ribeiro L, Lobo C. Phenotypes and biomarkers of diabetic retinopathy. *Prog Retin Eye Res*. 2014;41(1):90–111.
4. Lynch SK, Abràmoff MD. Diabetic retinopathy is a neurodegenerative disorder. *Vis Res*. 2017;139:101–107.
5. de Carlo TE, Romano A, Waheed NK, Duker JS. A review of optical coherence tomography angiography (OCTA). *Int J Retina Vitreous*. 2015;1(1):5.
6. Ong JX, Fawzi AA. Perspectives on diabetic retinopathy from advanced retinal vascular imaging. *Eye (Lond)*. 2022;36(2):319–327.
7. Ribeiro L, Marques IP, Santos T, et al. Characterization of two-year progression of different phenotypes of nonproliferative diabetic retinopathy. *Ophthalmic Res*. 2022;66(1):228–237.
8. Marques IP, Reste-Ferreira D, Santos T, et al. Progression of capillary hypoperfusion in advanced stages of nonproliferative diabetic retinopathy: 6-month analysis of RICHARD Study. *Ophthalmol Sci*. 2025;5(2):100632.
9. Santos T, Warren LH, Santos AR, et al. Swept-source OCTA quantification of capillary closure predicts ETDRS severity staging of NPDR. *Br J Ophthalmol*. 2022;106(5):712–718.
10. Nunes S, Pires I, Rosa A, Duarte L, Bernardes R, Cunha-Vaz J. Microaneurysm turnover is a biomarker for diabetic retinopathy progression to clinically significant macular edema: findings for type 2 diabetics with nonproliferative retinopathy. *Ophthalmologica*. 2009;223(5):292–297.
11. Bernardes R, Nunes S, Pereira I, et al. Computer-assisted microaneurysm turnover in the early stages of diabetic retinopathy. *Ophthalmologica*. 2009;223(5):284–291.
12. Mendes L, Rocha A, Lopes M, et al. Microaneurysm counting as a biomarker for the hyperperfusion stage of nonproliferative diabetic retinopathy. *Ophthalmol Ther*. 2025;14(8):1905–1915.
13. Ferris FL, Bailey I. Standardizing the measurement of visual acuity for clinical research studies: guidelines from the Eye Care Technology Forum. *Ophthalmology*. 1996;103(1):181–182.
14. Lei J, Durbin MK, Shi Y, et al. Repeatability and reproducibility of superficial macular retinal vessel density measurements using optical coherence tomography angiography en face images. *JAMA Ophthalmol*. 2017;135(10):1092–1098.
15. Durbin MK, An L, Shemonski ND, et al. Quantification of retinal microvascular density in optical coherence tomographic angiography images in diabetic retinopathy. *JAMA Ophthalmol*. 2017;135(4):370–376.
16. Foote KG, Roorda A, Duncan JL. Multimodal imaging in choroideremia. *Adv Exp Med Biol*. 2019;1185:139–143.
17. Li Y, El Habib Daho M, Conze PH, et al. Hybrid fusion of high-resolution and ultra-widefield OCTA acquisitions for the automatic diagnosis of diabetic retinopathy. *Diagnostics (Basel)*. 2023;13(17):2770.
18. Akman A, Meditec CZ. *Optical Coherence Tomography in Glaucoma: A Practical Guide*. Cham: Springer International Publishing; 2018.
19. Kakihara S, Hirano T, Kitahara J, et al. Application of optical coherence tomography angiography to assess systemic severity in patients with hereditary transthyretin amyloidosis. *PLoS One*. 2022;17(9):e0275180.
20. Altman DG. *Practical Statistics for Medical Research*. London: Chapman & Hall/CRC; 1990.

21. Marques IP, Ribeiro ML, Santos T, et al. Patterns of progression of nonproliferative diabetic retinopathy using non-invasive imaging. *Transl Vis Sci Technol*. 2024;13(5):22.
22. Waheed NK, Rosen RB, Jia Y, et al. Optical coherence tomography angiography in diabetic retinopathy. *Prog Retin Eye Res*. 2023;97:101206.
23. Kohner EM, Henkind P. Correlation of fluorescein angiogram and retinal digest in diabetic retinopathy. *Am J Ophthalmol*. 1970;69(3):403–414.
24. Takamura Y, Yamada Y, Inatani M. Role of microaneurysms in the pathogenesis and therapy of diabetic macular edema: a descriptive review. *Medicina (Kaunas)*. 2023;59(3):435.
25. Cogan DG, Kuwabara T. Capillary shunts in the pathogenesis of diabetic retinopathy. *Diabetes*. 1963;12(4):293–300.
26. Silva PS, Marcus DM, Liu D, et al. Association of ultra-widefield fluorescein angiography–identified retinal nonperfusion and the risk of diabetic retinopathy worsening over time. *JAMA Ophthalmol*. 2022;140(10):936–945.
27. Curtis TM, Gardiner TA, Stitt AW. Microvascular lesions of diabetic retinopathy: clues towards understanding pathogenesis? *Eye*. 2009;23(7):1496–1508.
28. Cunha-Vaz J, Mendes L, Reste-Ferreira D. Understanding nonproliferative diabetic retinopathy progression using noninvasive imaging. *Eye*. 2025;39(14):2627–2634.
29. Cunha-Vaz J, Mendes L. Characterization of risk profiles for diabetic retinopathy progression. *J Pers Med*. 2021;11(8):826.
30. Santos AR, Lopes M, Santos T, et al. Intraretinal microvascular abnormalities in eyes with advanced stages of nonproliferative diabetic retinopathy: comparison between UWF-FFA, CFP, and OCTA—the RICHARD Study. *Ophthalmol Ther*. 2024;13(12):3161–3173.
31. Levine ES, Arya M, Chaudhari J, et al. Repeatability and reproducibility of vessel density measurements on optical coherence tomography angiography in diabetic retinopathy. *Graefes Arch Clin Exp Ophthalmol*. 2020;258(8):1687–1695.
32. Lujan BJ, Calhoun CT, Glassman AR, et al. Optical coherence tomography angiography quality across three multicenter clinical studies of diabetic retinopathy. *Transl Vis Sci Technol*. 2021;10(3):2.